

A cryogenic scanning near-field optical microscope with shear-force gapwidth control

A. Kramer, J.-M. Segura, A. Hunkeler, A. Renn, and B. Hecht^{a)}
*Physical Chemistry Laboratory, Swiss Federal Institute of Technology, ETH-Zentrum,
CH-8092 Zurich, Switzerland*

(Received 26 November 2001; accepted for publication 13 May 2002)

We present a scanning near-field optical microscope designed for nanoscale optical imaging and spectroscopy as well as simultaneous tuning fork shear-force topographic imaging at cryogenic temperatures. The whole setup is immersed in superfluid helium ($T=1.8$ K). In this medium we observe resonance frequency fluctuations of the tuning fork sensor with an amplitude of $\Delta\nu\approx 5\%–10\%$ of the full width at half-maximum of the resonance. Possible reasons for the occurrence of the frequency fluctuations are discussed. A stable gapwidth feedback can still be achieved if the set value of the frequency shift is chosen slightly larger than the fluctuation amplitude. As an example we demonstrate shear-force topographic imaging of a silicon grating in superfluid helium. © 2002 American Institute of Physics. [DOI: 10.1063/1.1491028]

I. INTRODUCTION

Optical microscopy and spectroscopy at very low temperatures offers the unique possibility to undertake detailed spectroscopic studies on single molecules^{1,2} and quantum dots³ in the absence of any temperature-induced disturbances. However, the spatial resolution of optical microscopy at low temperatures is limited by diffraction and instrumental constraints. In recent single-molecule experiments at liquid-helium temperature using scanning confocal optical microscopy a lateral spatial resolution of $\Delta x\approx 800$ nm was achieved.⁴ Using scanning near-field optical microscopy (SNOM or NSOM) techniques, the lateral resolution can be significantly enhanced. In aperture SNOM, light is confined to a subwavelength spot by means of an aperture in the metal coating at the apex of a fiber probe.^{5–7} An alternative method, tip-enhanced SNOM, relies on the confined and enhanced optical fields at a sharp tip to generate contrast on a subwavelength scale.^{8–11} Besides the potential for enhanced spatial resolution, the combination of optical spectroscopy at cryogenic temperature and local probe techniques bears further exciting potential: (i) The narrow zero-phonon lines of single guest molecules are very sensitive probes for minute changes in their immediate environment.¹ However, it is often difficult to relate the observed line shifts and broadenings to the actual microscopic mechanisms in the matrix. A sharp probe can be used to perform local perturbation experiments on single molecules.¹² Such experiments can shed light on the subtle interactions that govern the low-temperature spectral dynamics of single molecules by providing high spatial resolution and by allowing to reversibly switch on and off a certain perturbation.¹² (ii) The presence of a metallic tip allows combining optical spectroscopy with electronic spectroscopy by investigating I/V curves and spectral behavior of certain nanostructures.¹³

In this article we present a cryogenic scanning near-field optical microscope with shear-force gapwidth control designed for operation at liquid-helium and room temperature. This apparatus allows performing single-particle perturbation experiments with solid metal tips, where excitation is performed in far field, as well as experiments with conventional aperture tips for near-field excitation.^{5–7} In the latter case a confocal optical system is used for efficient light collection and background-free detection. We demonstrate controlled tip-sample approach, gapwidth feedback, and shear-force topographic imaging at $T=1.8$ K.

II. SETUP

A. General description

The microscope setup consists of a scan head placed on top of a sample-scanning confocal optical microscope, described previously.⁴ The scan head is sketched in Fig. 1. In order to correlate the tip-sample interaction with the optical response of the sample, it is necessary that the optical detection system's focus coincides with the tip-sample interaction area. This requires that the tip can be positioned relative to the optical focus in three dimensions. To accomplish this, coarse $x-y$ positioning of the tip is performed by moving the whole scan head laterally. This scan head translation is achieved by an inertia drive.^{4,14–16} Motion is induced by three stacks of shear piezos (SPs). Each stack consists of two piezos separated by an insulating layer. The orientations of the two piezos in the stack differ by 90° (one piezo for the x , one for the y direction). The stacks are equidistantly distributed on a circle, while having the same orientation. The sliding surface is defined by the contact points between sapphire balls (SBs) glued onto the shear piezo stacks and sapphire plates (SAs) attached to the scan head. The minimal voltage applied on the actuator, which is needed to produce a translational motion is determined by the mass of the whole actuator-load system. Therefore, the overall mass of the probe scan head has been kept as low as possible. In the

^{a)}Corresponding author; present address: Nano-Optics Group, Institute of Physics, University of Basel; electronic mail: bert.hecht@nano-optics.ch

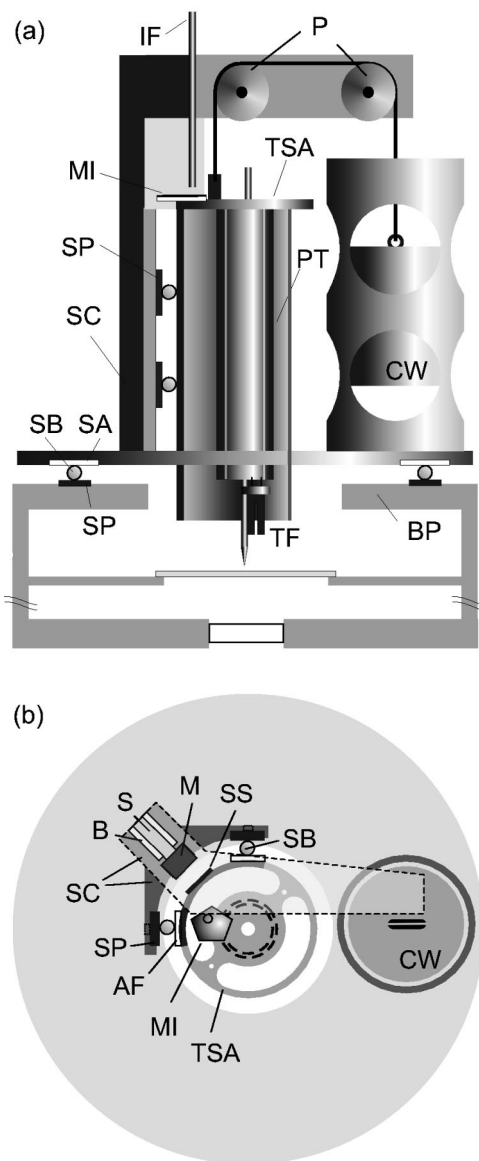


FIG. 1. Scheme of the scan head in side view (a) and top view (b): (TSA) tube scanner assembly, (PT) piezo tube, (TF) tuning fork, (SC) static counterpart, (BP) base plate, (SP) shear piezo stack, (SB) sapphire ball, (SA) sapphire plate, (IF) interferometer fiber, (MI) mirror, (P) pulley, (CW) counter weight, (B) bearing, (S) screw, (M) magnet, (SS) steel sheet, (AF) aluminum plane face.

present design, a movement can be achieved reproducibly using a saw-tooth voltage of 600 V amplitude at a frequency of 800 Hz. At room temperature a lateral speed of approximately 0.5 mm/s can be achieved. This corresponds to a step size of up to 600 nm. At $T=1.8$ K the step size is lowered by a factor of 10.

B. Probe preparation

The preparation of aperture probes is performed according to standard procedures.¹⁷ The end of a single-mode glass fiber (FS-SN-3224 from 3M) is dipped into a 40% concentrated HF solution for 130 min. The resulting tip is very sharp with a typical taper angle of 20°. Finally, in order to be able to apply an electric field on the tip, a 20-nm-thick gold

coating is sputtered onto the fiber end. Our experiments with gold-coated tapered glass tips are reported elsewhere.¹² In the present article only solid gold tips are used. They are manufactured by electrochemical etching of a thin wire with a diameter of 20 μm . Tips are etched in HCl (25%) at an ac voltage of between 1 and 2 V at a frequency of 50 Hz.¹⁸ The tips are attached to one arm of the tuning fork with super glue or two-component epoxy glue. The tuning forks used were standard 32.768 kHz resonators with an arm size of $4 \times 0.6 \times 0.4$ mm³.

III. COARSE AND FINE APPROACH OF THE TIP

A critical task is the vertical approach of the tip to the sample. While for lateral positioning the whole scan head is shifted, in the vertical direction only a smaller element, the tube scanner assembly (TSA), is moved (see Fig. 1). It mainly consists of a piezo tube (PT) with the tuning fork (TF) and its support. Here again the inertia drive principle is applied. However, gravity causes an anisotropy between the upwards and downwards motion. This problem is solved by using a counterweight (CW) to compensate for the weight of the TSA (see Fig. 1). Using a pulley (P), the TSA is almost exactly counterbalanced by a slightly heavier weight. Thus, uncontrolled movement of the assembly will result in an upwards motion. The pulley consists of two disks with a V-shaped groove on their rim. The disks can freely rotate with enough looseness to avoid thermal constriction on cooling. The thread connecting the TSA and the counterweight is made of Kevlar to ensure combined high mechanical strength and flexibility even at low temperature. Figure 1 also illustrates how the movable TSA is attached to its static counterpart (SC). Magnets (M) glued on small screws are affixed to the vertical beam of the SC. We use strong NdFeB magnets that attract a thin steel sheet (SS) of the TSA. By varying the number of magnets (typically two) and their distance to the steel sheet, the attraction force, related linearly to the friction force, can be precisely adjusted. The two side wings of the vertical beam of the SC each carry two shear piezos (SP), respectively, oriented along the vertical axis (see Fig. 1). A small sapphire ball (SB) is glued on each shear piezo. Two aluminum plane faces (AF) down the side of the TSA rest on three of the sapphire balls. Long displacements of the TSA, which move the center of magnetic force out of the contact point triangle, may change its equilibrium resting position. Therefore, an additional fourth ball that serves as a spare contact point is implemented. Its height can be adjusted by a screw.

The whole setup consisting of the sample scanning confocal microscope and the tip scan head comprises remote control over six degrees of freedom for fine positioning and five degrees of freedom for coarse positioning of the tip and the sample.

Approaching a tip to the sample in superfluid helium (He II) is difficult, since in the present setup no visual control of the coarse approach is possible. For example, the z motion of the TSA can occasionally be blocked if the slipping is hindered by small dust particles or by microgrooves on the sliding surfaces. Therefore, a method for monitoring the mo-

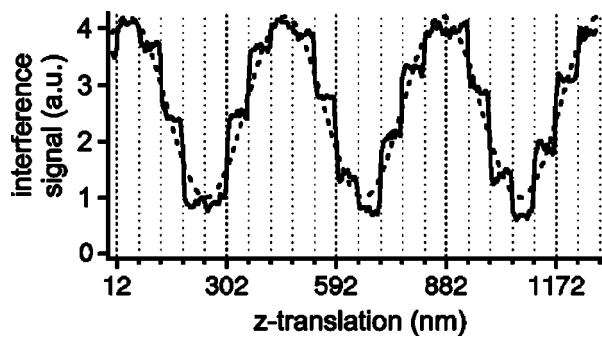


FIG. 2. Interference signal for monitoring the coarse z motion of the tube scanner assembly (TSA) at room temperature. The TSA acts as a movable mirror of one arm of an interferometer. The plot shows the interferometer signal vs z displacement when moving the TSA. The solid line reflects the actual slip-stick motion of the TSA with discrete steps of ≈ 58 nm. The sinusoidal fit (dashed) represents the theoretical case of a linear continuous motion of the TSA. The interferometer employs a 830 nm laser diode.

tion of the TSA has been implemented. If the z translation once has stopped, it is possible to continue the approach by moving back several steps and then forth again. A reliable monitor signal of the TSA motion is provided by the change of the optical path between a mirror (MI) attached to the TSA and the flat fiber end (IF) of a fiber interferometer (wavelength 830 nm, Fiber: 3M FS-SSC5624, single mode, $\lambda_{\text{cutoff}} = 864$ nm), [see Fig. 1(a)]. A typical approach experiment at room temperature is plotted in Fig. 2. The offset-corrected interferometer signal, reflecting the stepwise coarse motion of the TSA, is displayed. In general, signal modulation of approximately 15% of the total signal is easily achieved. The typical distance between fiber and mirror is 1–2 mm. The sinusoidal fit (dashed line) represents the signal, which would have been measured if the z motion was a linear continuous z translation. The high reproducibility of equidistant steps of $\Delta z \approx 58$ nm is evident. The step width can be adjusted by varying the amplitude of the voltage ramp applied to the shear piezos. However, there is a threshold below which the motion stops due to insufficient acceleration for the slipping process. At liquid-helium temperature the required voltage for a certain step width is a factor of 5–10 larger than compared to room temperature operation.

The fine approach of the tip in conventional scanning probe microscopy is generally performed using a short-range signal such as a tunneling current or van der Waals interaction forces. In our setup we have implemented a quartz tuning fork as shear force sensor.¹⁹ Here the tip is attached to one arm of a fork that oscillates close to its resonance frequency (≈ 32.7 kHz). Since both excitation and detection of the resonance is performed by the fork element itself, no alignment is required at 1.8 K. The successful operation of a similar configuration in a gas cryostat operated at 1.8 K has been demonstrated previously.²⁰ Approaching the tip to the sample surface results in a shift of the resonance frequency to higher frequencies (typically $\Delta\nu/\nu \approx 10^{-5}$ Hz for gold wires with a length of 2 mm glued to a 32.768 kHz fork). The length of the excess end with tip is ~ 0.25 mm. Detecting the shift with a lock-in technique and using, e.g., the phase signal as input for a feedback loop enables us to ap-

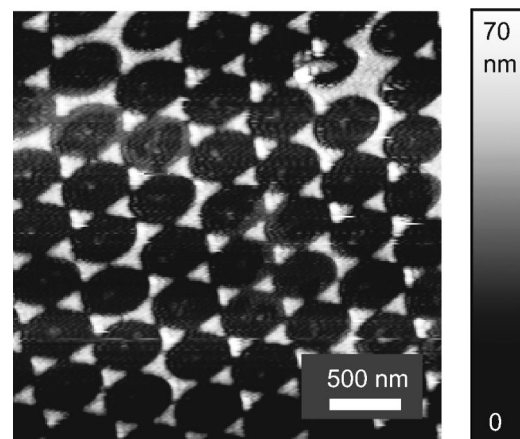


FIG. 3. Topographic imaging with shear-force distance control at room temperature. The investigated sample consists of a hexagonal pattern of small Al islands with a height of 20 nm on a glass surface. The distortion-free image evidences stable scan conditions (image size: 239×239 pixels, scan speed 15 ms/pixel).

proach the tip in a controlled way to the sample and to scan the surface.

IV. EXPERIMENTS AND RESULTS

The performance of the shear-force feedback has been tested at room temperature first, using an electrochemically etched gold tip. As an example a topographic image of a hexagonal pattern of small Al islands on glass²¹ is presented in Fig. 3. The image shows that the hexagonal pattern is well reproduced proving that the shear-force topographic imaging with this setup is stable and reliable.

Unexpectedly, when having the tip-tuning-fork system immersed in superfluid helium at $T = 1.8$ K, random fluctuations of the resonance frequency appear, independent of the distance of the tip to the sample. In Fig. 4 the lock-in phase signal of the fork oscillation versus time is plotted. In the

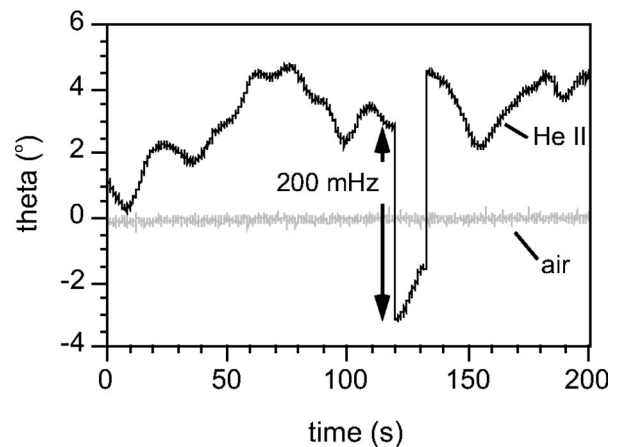


FIG. 4. Resonance frequency fluctuation reflected by the phase of the tuning fork oscillation at resonance, in air (gray) and in superfluid helium (black). For calibration purposes a change of the excitation frequency of 200 mHz was applied at $t = 120$ s and back to the old value at $t = 132$ s. This allows us to estimate the range of resonance frequency fluctuation to be approximately 150 mHz. (The time constant of the lock-in was $300 \mu\text{s}$, which is much smaller than the characteristic time constant of the phase fluctuation.)

first approximation, at resonance, a small phase variation is proportional to the frequency shift. Thus, monitoring the phase signal provides direct information about the resonance frequency fluctuation. From Fig. 4 it can be recognized that in air (gray line) no resonance frequency fluctuation occurs, whereas in superfluid helium (black line) the variation corresponds to approximately 150 mHz [the full width at half-maximum (FWHM) of the resonance of this tip/fork assembly is 3.5 Hz]. From further experiments we know that the amplitude of the fluctuation is generally between 5%–10% of the FWHM of the resonance. The manually induced shift of the curve at $120\text{ s} < t < 135\text{ s}$ in Fig. 4 is due to a sudden change of the excitation frequency by 200 mHz. In this way a calibration of the phase-frequency relation is obtained.

However, despite the resonance instability in He II, it is possible to exploit the resonance frequency shift of the tuning fork sensor when approaching the sample for shear-force feedback operation. In the constant phase mode, the difference between set point and the value of free vibration has to be chosen larger than the fluctuation amplitude. There exist few reports about tip-sample distance regulation for SNOM where the whole setup is immersed in superfluid helium.^{22,23}

However, to our knowledge, shear-force topographic imaging has not been presented so far. We show in Fig. 5 the first images generated with our setup. The images were obtained with tuning fork shear-force feedback in constant phase mode at a temperature of 1.8 K. The sample, a silicon line grating, is scanned in the x - y direction while the gold tip is moved in the z direction. A schematic cross section of the sample is depicted at the top of Fig. 5(a). The line pattern of the grating is well reproduced by the SNOM, however, the grooves appear slightly narrower than the elevations. This effect arises from a convolution of the sample profile with the tip shape. Accordingly, if either the cone angle of the tip or the step height of the grating is large, it is expected that elevations of the sample appear wider in the topographic image. The apparent noise in Fig. 5(a) is most likely due to slight feedback loop oscillations. The latter can arise from a high set-frequency shift, which in our case is required to circumvent the problem of resonance frequency fluctuation. In the upper half of Fig. 5(a), slight depressions on the elevations of the grating can be recognized. These features are also present in the backward scan image and consequently are not due to spontaneous imaging disturbances. Prior to the sample scan we performed two $2\text{ }\mu\text{m}$ scans at different locations in this area of the sample. The appearance of a lower average height level in a certain region is also evident in the upper half of Fig. 5(b). Previous to Fig. 5(b) we performed a $12\text{ }\mu\text{m} \times$ linescan followed by a $12 \times 9\text{ }\mu\text{m}^2$ x/y scan. These observations lead to the assumption that the apparent depressions in the topography are most likely due to a kind of surface modification induced in a previous scan. Since it is unlikely that the soft gold tip removes some material of the silicon oxide at the surface of the silicon grating, we believe that the tip modifies a thin contamination layer present on the surface of the grating. It is well known that the shear-force interaction also depends on the chemical properties of the tip and sample surface and thus can result in a topographic contrast. The origin of the surface modification is not yet clear to

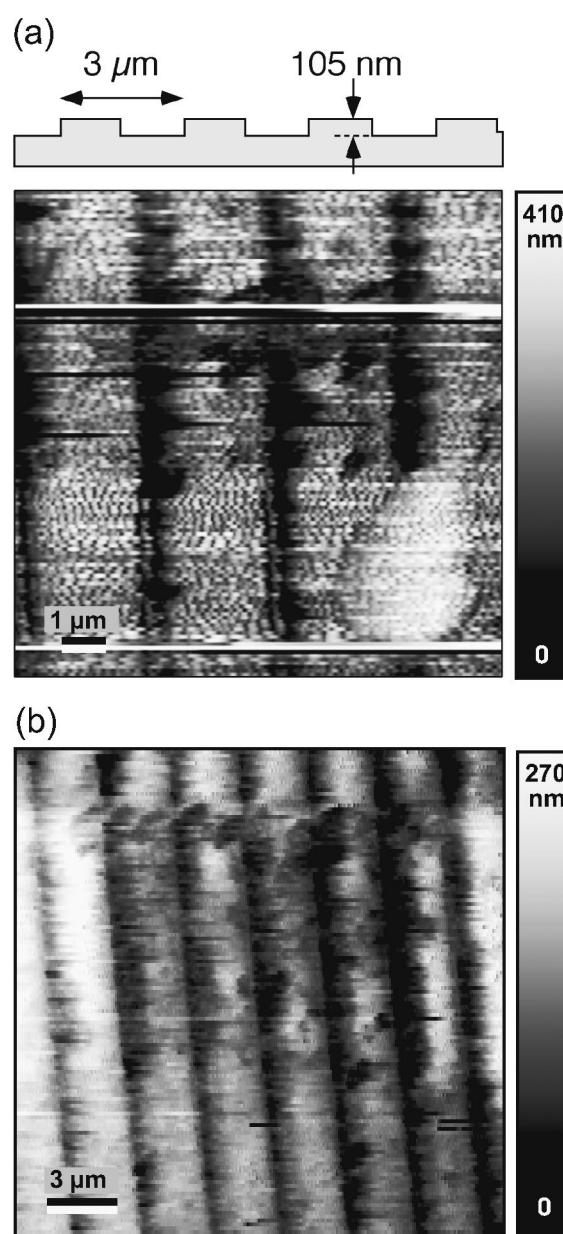


FIG. 5. Topographic imaging in superfluid helium at $T = 1.8\text{ K}$. The sample is a silicon line grating with the lines oriented perpendicular to the fast scans direction (top panel). The weakly bound dust particle at bottom right of image (a) indicates that the scan process can be performed in a controlled way while the interaction forces are in a favorable regime. In the upper half of the image (b), the average topography level appears lower in an area of $12 \times 9\text{ }\mu\text{m}^2$, possibly due to a surface modification of the grating. The seemingly elevated regions at the left and right margins of this area are an artifact of the line-by-line background subtraction. Both images: 256×256 pixels, scan speed 23 ms/pixel .

us. Similar effects could not be observed at room temperature so that the modifications are likely related to the presence of superfluid helium.

Note that the resonance frequency fluctuations of the tuning fork imply a varying interaction force between tip and sample during the scan. However, the range of interaction forces still seems to be favorable for the successful imaging of structures, which are only loosely bound to the grating's surface. This is demonstrated by the successful reproducible imaging of a small dust particle at the right lower part of Fig. 5(a).

V. DISCUSSION

The origin of the resonance fluctuations of the tuning fork in superfluid helium is not yet clear. We speculate, that one possible reason is a temperature fluctuation in the He II phase. This would affect both the viscosity of the surroundings and the actual temperature of the tuning fork, consequently causing a resonance frequency shift. Thermodynamic instabilities have also been mentioned as a possible reason by Rychen *et al.*, who have observed a similar phenomenon for a tuning fork in superfluid helium.²⁴ The temperature of the He II phase is unambiguously related to the vapor pressure. At our working point ($T=1.8$ K) we find a temperature-pressure relation of $\Delta p/\Delta T \approx 60$ mbar/K. From a calibration of the tuning fork resonance frequency vs pressure, we know that the observed fluctuation would correspond to a pressure fluctuation of $\Delta p \approx 3$ mbar (or correspondingly $\Delta T \approx 50$ mK). (This means, on the other hand, that a tuning fork could obviously be used as a very precise thermometer in the mK regime.) We assume that instabilities of the suction rate of our pump are responsible for the temperature fluctuation. A change in vapor pressure at the free surface of the liquid helium would then cause (i) an instantaneous temperature change of the whole liquid in a first approximation, or (ii) temperature waves propagating through it (second sound). Moreover one could think of the formation of a standing second sound wave in the cryostat. The geometric arrangement of the standing wave pattern depends on the boundaries of the cavity, e.g., on the free surface of the liquid He. If there is also a surface wave pattern changing with time, the standing wave in the bulk will be modified. In order to check the above discussed assumptions, in future experiments a thermometer will be implemented in the liquid-helium phase.

In conclusion, we have discussed the design and implementation of a low temperature SNOM. The apparatus is in particular designed for optical investigation of single particles, like molecules and quantum dots. We demonstrate shear-force topographic imaging of a silicon grating in superfluid helium. The possibility of *in situ* coarse positioning of the tip and shear-force gapwidth control will enable controlled near-field experiments in combination with single-particle spectroscopy at 1.8 K.

ACKNOWLEDGMENTS

Special thanks go to B. Lambillotte for excellent mechanical support. The authors are grateful to Professor U. P. Wild for continuous help and support. This project was funded by the Swiss National Science Foundation (NFP 36) and the ETH Zürich.

- ¹T. Basché, W. E. Moerner, M. Orrit, and U. P. Wild, *Single-Molecule Optical Detection, Imaging and Spectroscopy* (VCH Verlagsgesellschaft, Weinheim/Germany, 1997).
- ²W. E. Moerner and M. Orrit, *Science* **283**, 1670 (1999).
- ³A. P. Alivisatos, *Science* **271**, 933 (1996).
- ⁴J.-M. Segura, A. Renn, and B. Hecht, *Rev. Sci. Instrum.* **71**, 1706 (2000).
- ⁵D. W. Pohl, W. Denk, and M. Lanz, *Appl. Phys. Lett.* **44**, 651 (1984).
- ⁶A. Harootunian, E. Betzig, M. Isaacson, and A. Lewis, *Appl. Phys. Lett.* **49**, 674 (1986).
- ⁷E. Betzig, J. K. Trautmann, T. D. Harris, J. S. Weiner, and R. L. Kostelak, *Science* **251**, 1468 (1991).
- ⁸Y. Inoué and S. Kawata, *Opt. Lett.* **19**, 159 (1994).
- ⁹F. Zenhausern, Y. Martin, and H. K. Wickramasinghe, *Science* **269**, 1083 (1995).
- ¹⁰B. Knoll and F. Keilmann, *Nature (London)* **399**, 134 (1999).
- ¹¹A. Kramer, W. Trabesinger, B. Hecht, and U. P. Wild, *Appl. Phys. Lett.* **80**, 1652 (2002).
- ¹²J.-M. Segura, G. Zumofen, A. Renn, B. Hecht, and U. P. Wild, *Chem. Phys. Lett.* **340**, 77 (2001).
- ¹³U. Banin, Y. Cao, D. Katz, and O. Millo, *Nature (London)* **400**, 542 (1999).
- ¹⁴G. Mariotto, M. D'Angelo, and I. V. Shvets, *Rev. Sci. Instrum.* **70**, 3651 (1999).
- ¹⁵C. L. Jahncke and H. D. Hallen, *Rev. Sci. Instrum.* **68**, 1759 (1997).
- ¹⁶D. V. Pelekhov, J. B. Becker, and G. Nunes, *Appl. Phys. Lett.* **72**, 993 (1998).
- ¹⁷R. Stöckle, C. Fokas, V. Deckert, R. Zenobi, B. Sick, B. Hecht, and U. P. Wild, *Appl. Phys. Lett.* **75**, 160 (1999).
- ¹⁸Y. D. Suh, V. Deckert, and R. Zenobi (personal communication, 2000).
- ¹⁹K. Karrai and R. D. Grober, *Appl. Phys. Lett.* **66**, 1842 (1995).
- ²⁰J. Rychen, T. Ihn, P. Studerus, A. Herrmann, K. Ensslin, H. J. Hug, P. J. A. van Schendel, and H. J. Güntherodt, *Appl. Surf. Sci.* **157**, 290 (2000).
- ²¹U. C. Fischer and H. P. Zingsheim, *J. Vac. Sci. Technol.* **19**, 881 (1981).
- ²²M. J. Gregor, S. Grosse, P. G. Blome, and R. G. Ulbrich, in *Photons and Local Probes*, edited by O. Marti and R. Möller (Kluwer Academic, Dordrecht, the Netherlands, 1995), pp. 133–138.
- ²³R. D. Grober, T. D. Harris, J. K. Trautman, and E. Betzig, *Rev. Sci. Instrum.* **65**, 626 (1994).
- ²⁴J. Rychen, T. Ihn, P. Studerus, A. Herrmann, and K. Ensslin, *Rev. Sci. Instrum.* **70**, 2765 (1999).